Supplementary Information:

Kinetic Partitioning with Effective Mass Accommodation for Secondary Organic Aerosol Simulations in Chemical Transport Modeling

Table S1. Molecular weight (MW) and T_g for oxidation products in volatility bins. Values of MW and T_g correspond to the respective volatility bin.

	TSOA (Pai et al., 2020)	ASOA (Pai et al., 2020)
C^0 (μg m^{-3})	0.1 1 10 100	10^{-10} 1 10 100

	TSOA (Shiraiwa et al., 2014)	ASOA (Shiraiwa et al., 2014; Shiraiwa et al., 2017)	LVOCOA (Shiraiwa et al., 2014)	SOAGX (Shiraiwa et al., 2014)
MW (g mol^{-1})	260 240 220 200	400 362 249 227	240	150

	TSOA	ASOA	LVOCOA	SOAIE (Chen et al., 2023)	SOAGX
T_g (K)	304 289 273 257	345* 289 273 256	314	231	261

T_g's calculated with T_g equation (Eq. (8)) except for SOAIE which was prescribed.

*Note that the volatility used to calculate the T_g for ASOAN is 10^{-4} μg m^{-3} in line with our previous study.

Table S2. Global averages of percent differences in SOA budget (between the α_{eff} kinetic and base case partitioning scheme simulations).

	Annual (%)	Winter (DJF) (%)	Spring (MAM) (%)	Summer (JJA) (%)	Autumn (SON) (%)
500 hPa	+14.56	+13.02	+14.31	+16.53	+15.97
850 hPa	1.43	+1.28	+1.78	+1.10	+1.97
Surface	-0.17	-0.03	+0.06	-0.06	+0.17
Total Column	-15.95	-17.57	-17.28	-15.10	-12.86

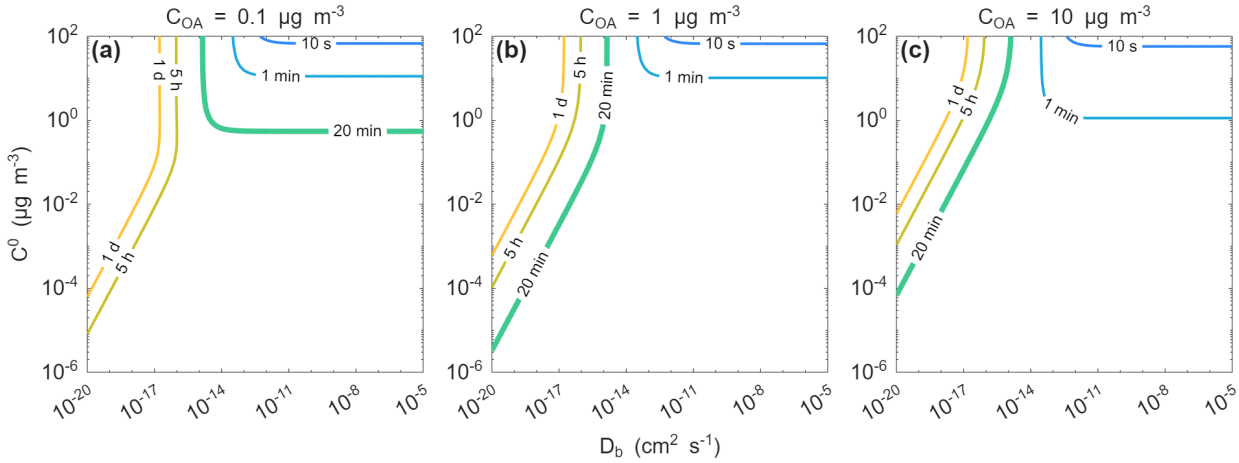

Figure S1. Contour plot of equilibration timescale (τ_{eq}) calculated using the approximate solution as a function of bulk diffusivity (D_b), saturation mass concentration (C^0), and initial pre-existing particle concentrations (C_{OA}) of (a) 0.1 μg m^{-3}, (b,) 1 μg m^{-3}, and (c) 10 μg m^{-3}. The equilibration timescale is calculated using the approximate solution. The initial gas-phase concentration was 0.1 μg m^{-3} and the temperature was set to 298K.

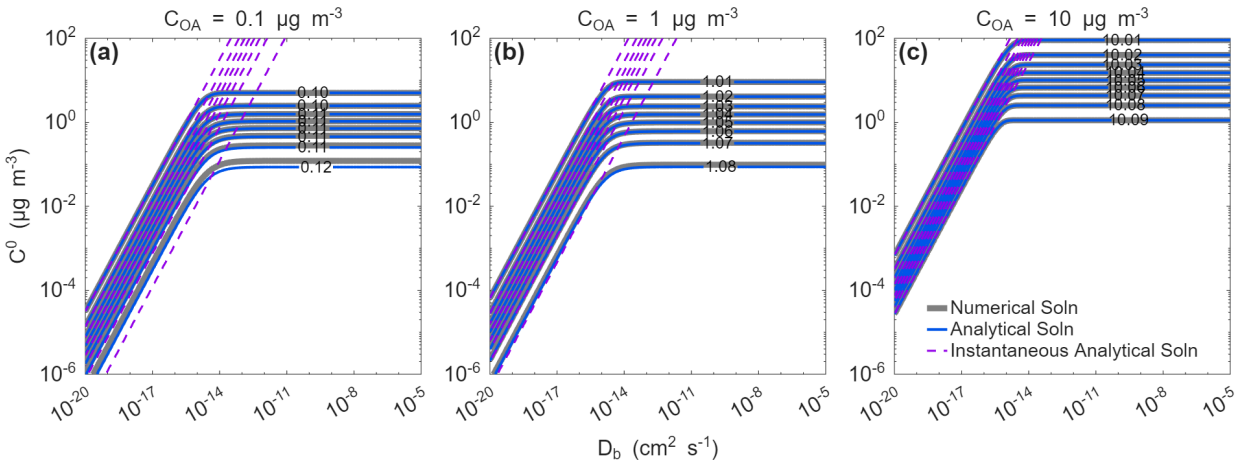

24

25 **Figure S2.** Contour plot of the final (t = 1200s) particle-phase concentration calculated using the
26 (1) numerical, (2) analytical, and (3) analytical solution using the instantaneous conditions as a
27 function of bulk diffusivity (D_b), saturation mass concentration (C^0), and initial pre-existing
28 particle concentrations (C_{OA}) of (a) 0.1 µg m^{-3}, (b,) 1 µg m^{-3}, and (c) 10 µg m^{-3}. The initial gas-
29 phase concentration was 0.1 µg m^{-3} and the temperature was set to 298K.

30

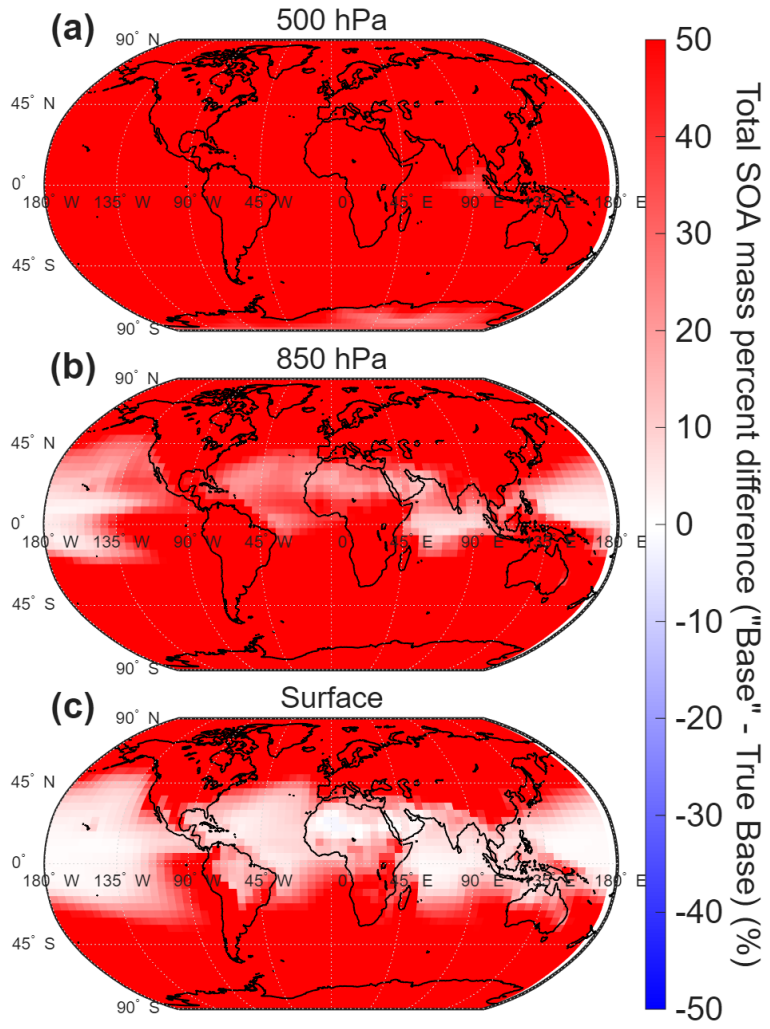

Figure S3. Annually averaged predicted percent SOA mass loading differences (a) at 500 hPa, (b) at 850 hPa, and (c) at the surface between the "Base" case partitioning scheme and the True Base simulations.

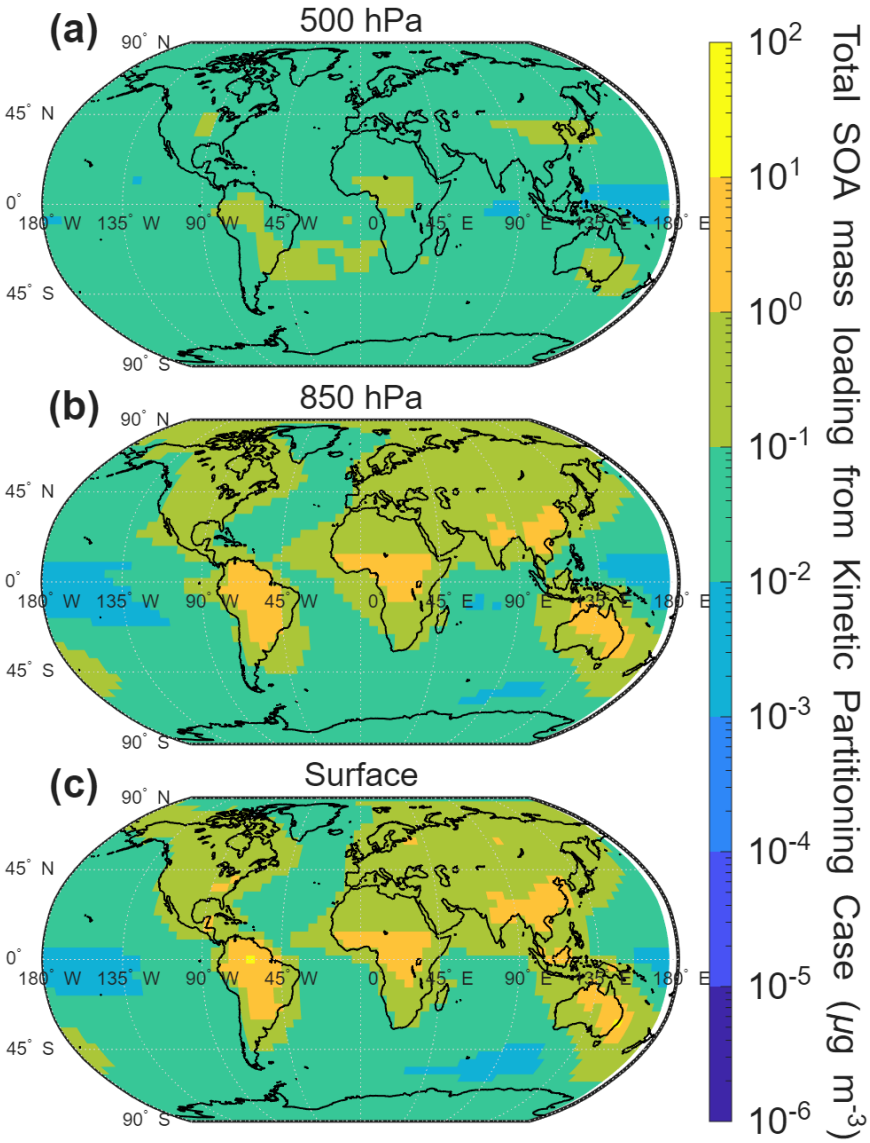

Figure S4. Predicted annual SOA budget (a) at 500 hPa, (b) at 850 hPa, and (c) at the surface using the α_{eff} kinetic partitioning scheme.

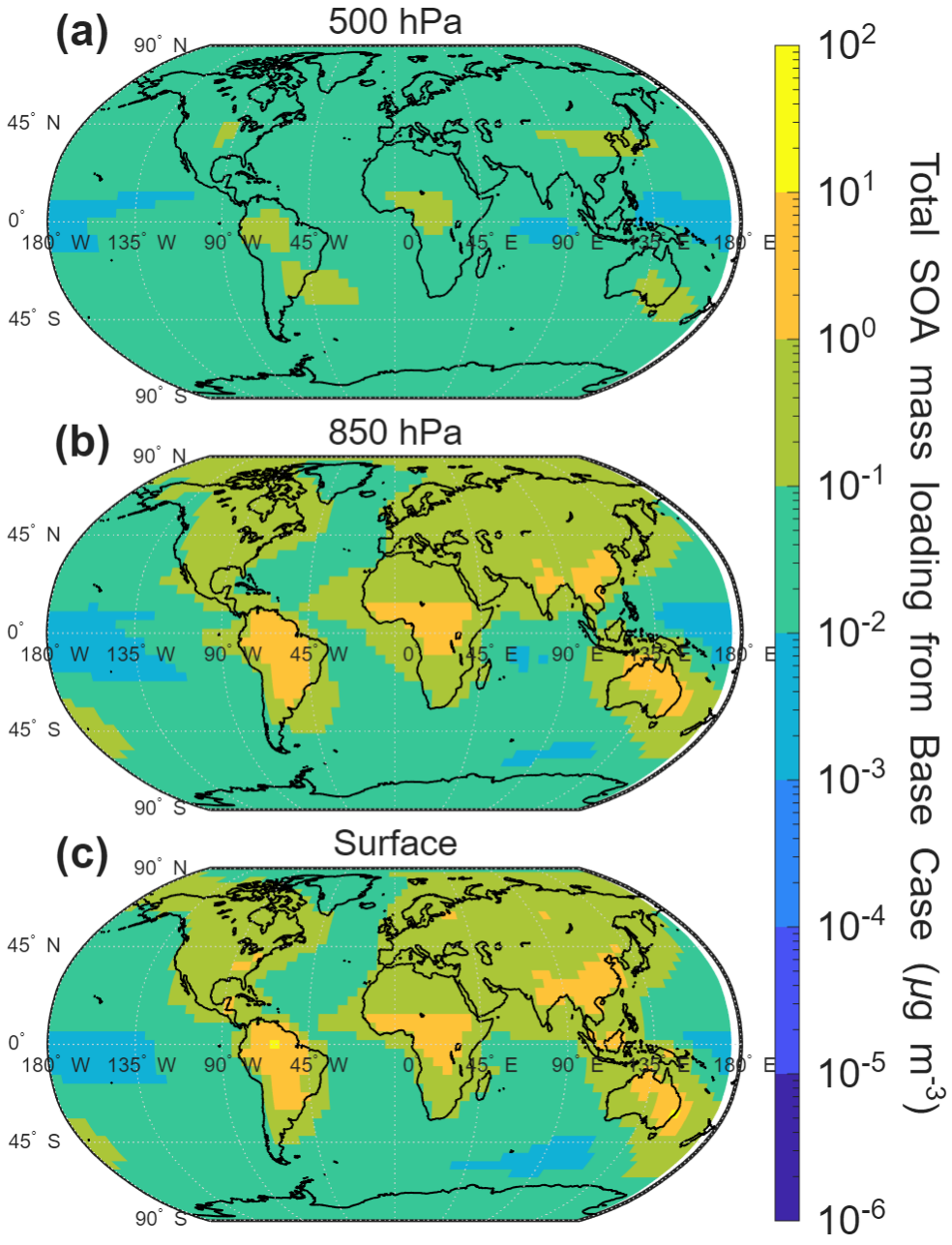

Figure S5. Predicted annual SOA budget (a) at 500 hPa, (b) at 850 hPa, and (c) at the surface using the Base case partitioning scheme.

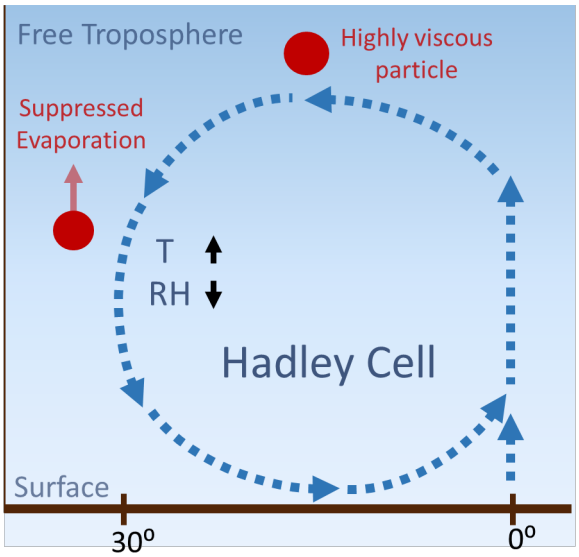

Figure S6. Schematic of Hadley Cell lifting highly viscous particles to the upper troposphere and transporting particles lower in altitude which would experience suppressed evaporation.

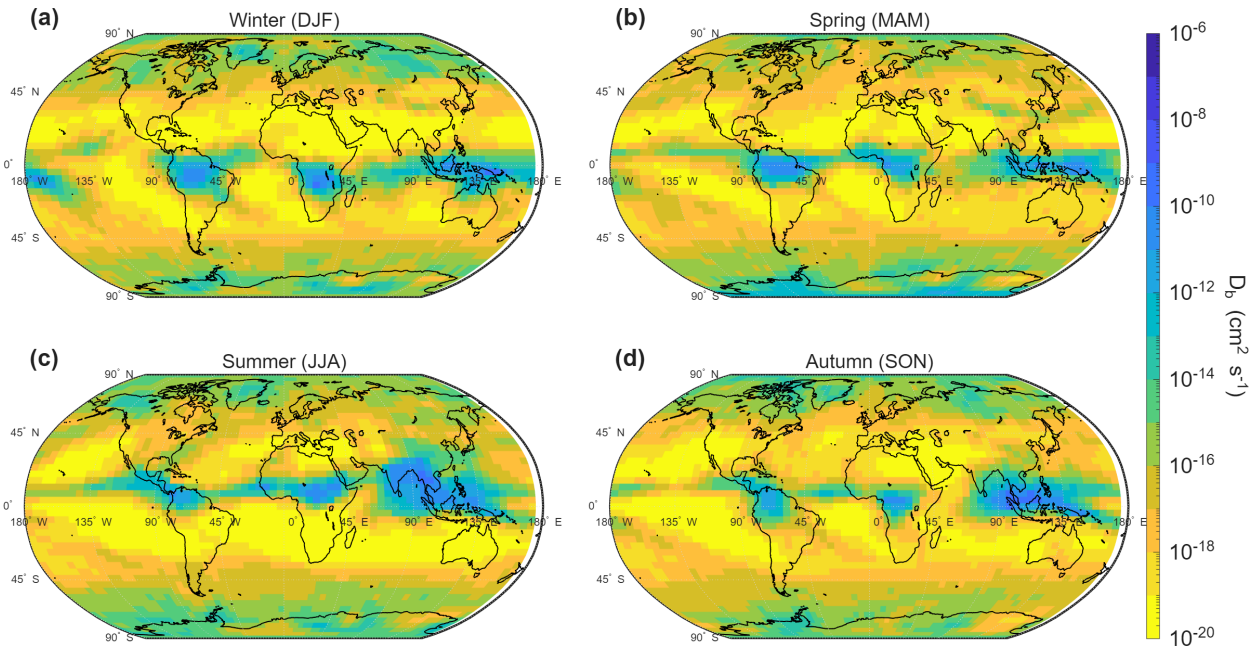

Figure S7. Predicted seasonal bulk diffusivities at 500 hPa.

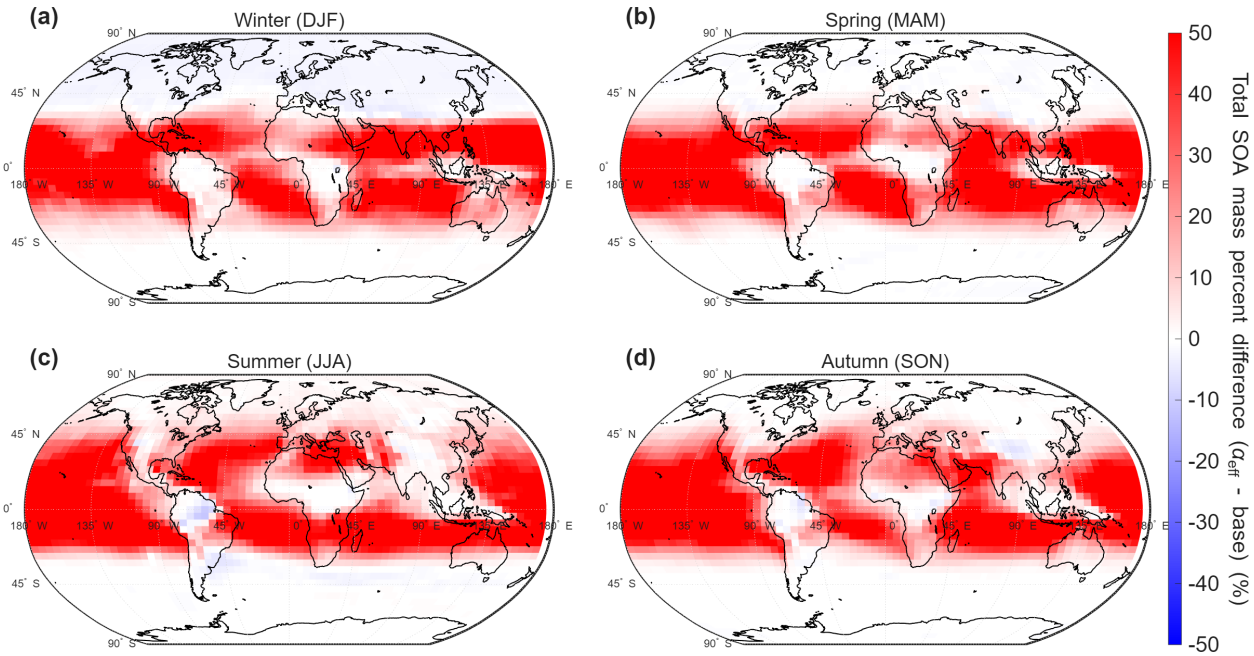

Figure S8. Predicted seasonal percent SOA budget differences at 500 hPa.

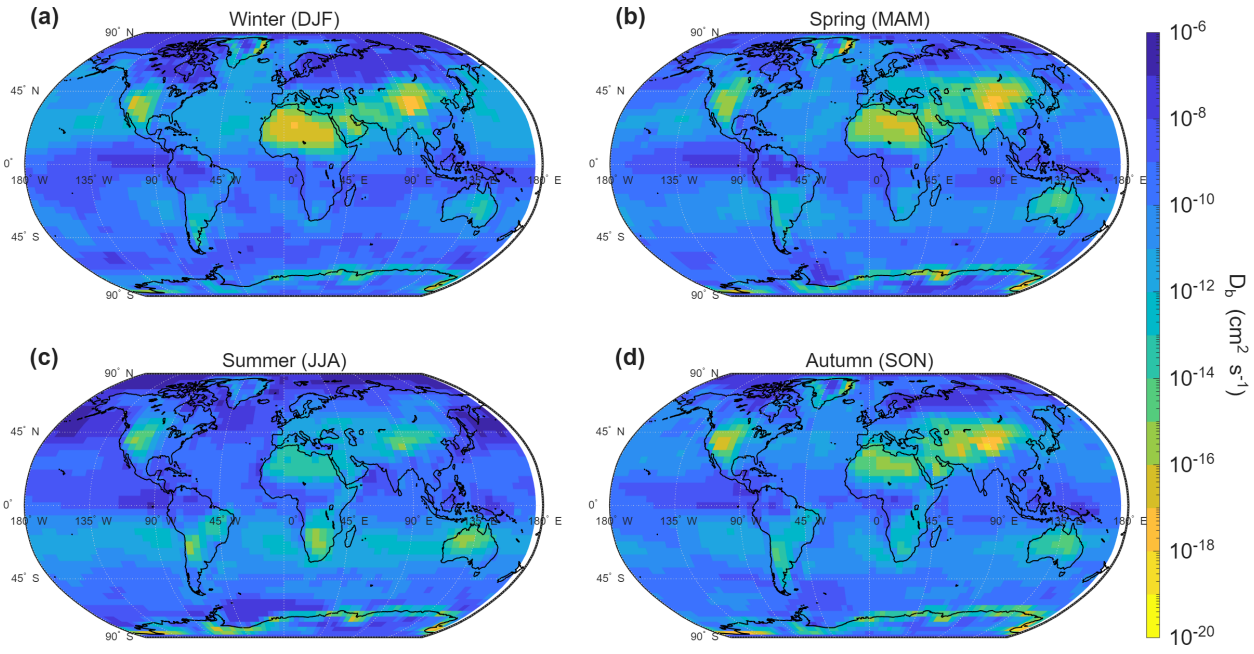

Figure S9. Predicted seasonal bulk diffusivities at the surface using the α_{eff} scheme.

References

Chen, B., Mirrielees, J. A., Chen, Y., Onasch, T. B., Zhang, Z., Gold, A., Surratt, J. D., Zhang, Y., & Brooks, S. D. (2023). Glass Transition Temperatures of Organic Mixtures from Isoprene Epoxydiol-Derived Secondary Organic Aerosol. The Journal of Physical Chemistry A, 127(18), 4125–4136. https://doi.org/10.1021/acs.jpca.2c08936

Pai, S. J., Heald, C. L., Pierce, J. R., Farina, S. C., Marais, E. A., Jimenez, J. L., Campuzano-Jost, P., Nault, B. A., Middlebrook, A. M., Coe, H., Shilling, J. E., Bahreini, R., Dingle, J. H., & Vu, K. (2020). An evaluation of global organic aerosol schemes using airborne observations. Atmospheric Chemistry and Physics, 20(5), 2637–2665. https://doi.org/10.5194/acp-20-2637-2020

Shiraiwa, M., Berkemeier, T., Schilling-Fahnestock, K. A., Seinfeld, J. H., & Pöschl, U. (2014). Molecular corridors and kinetic regimes in the multiphase chemical evolution of secondary organic aerosol. Atmospheric Chemistry and Physics, 14(16), 8323–8341. https://doi.org/10.5194/acp-14-8323-2014

Shiraiwa, M., Li, Y., Tsimpidi, A. P., Karydis, V. A., Berkemeier, T., Pandis, S. N., Lelieveld, J., Koop, T., & Pöschl, U. (2017). Global distribution of particle phase state in atmospheric secondary organic aerosols. Nature Communications, 8(1), 15002. https://doi.org/10.1038/ncomms15002